Supporting Information

Microwave and traditional solvothermal syntheses, crystal structures, mass spectroscopy and magnetic properties of $Co^{II}_4O_4$ cubes

Kun Zhang,[a] Jun Dai,[a] Yun-Hong Wang,[a] Ming-Hua Zeng,[*a, b] and Mohamedally Kurmoo[*c]

[a] Key Laboratory of Synthetic and Natural Functional Molecule Chemistry of the Ministry of Education, Northwest University, Xi'an, 710069; P. R. China. [b] Department of Chemistry and Chemical Engineering, Guangxi Normal University, Key Laboratory for the Chemistry and Molecular Engineering of Medicinal Resources (Ministry of Education) Guilin, 541004, P. R. China. [c] Laboratoire DECOMET, Institut de Chimie de Strasbourg, Université de Strasbourg, CNRS-UMR 7177, 4 rue Blaise Pascal, CS 90032, 67081 Strasbourg Cedex, France

Figure S11. Plots of χ^{-1}_{m} *vs.* *T* and the fit of Curie-Weiss law of **1** and **2** for different ranges of temperatures.
Figure S12. Plots of in-phase (χ') and out-of-phase (χ'') ac susceptibilities for **1** and **2**.

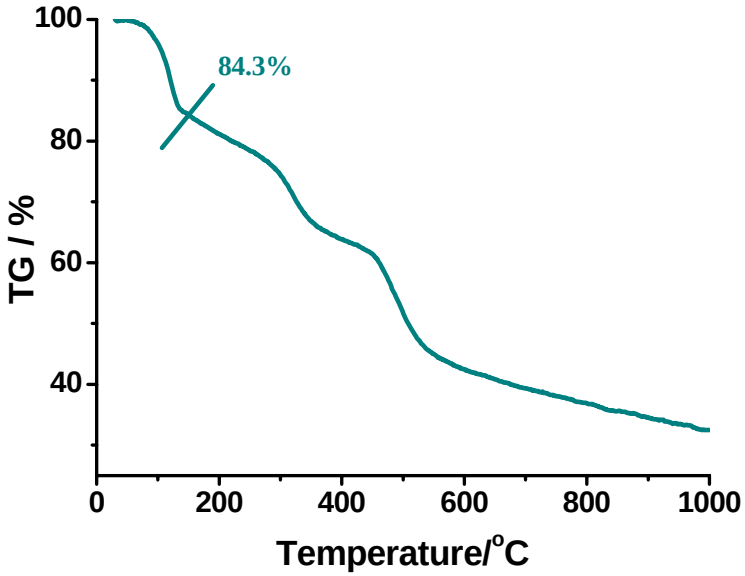

Figure S1. TG analysis was performed to confirmed the presence of guest molecule in **2**: TG measurement under N_2 atmosphere was performed by using a crushed ~~single~~ crystalline sample of **2** indicated loss of four terminal coordinated and two guest methanol molecules between 30 and 150 °C (15.7% mass loss observed, 15.8% calculated). Combined with the elemental analyses (see the experimental part) and the structural data, the final composition of **2** was determined as $[Co_4(heb)_4(\mu_3\text{-}OMe)_4(MeOH)_4]\cdot 2MeOH$.

Table S1 Selected bond lengths (Å) and angles (°) for **1** and **2**

1		**2**	
Co1-O1	2.086(2)	Co1-O1	2.068(3)
Co1-O(2)	2.027(2)	Co1-O2	2.022(3)
Co1-O4	2.051(2)	Co1-O4	2.116(3)
Co1-O5	2.157(3)	Co1-O5	2.140(3)
Co1-O4^a	2.084(2)	Co1-O4^a	2.052(3)
Co1-O4^b	2.129(2)	Co1-O4^b	2.081(2)
Co1-O4-Co1^b	98.50(9)	Co1-O4-Co1^a	99.7(1)
Co1-O4-Co1^c	97.56(8)	Co1-O4- Co1^c	94.6(1)
Co1^b-O4-Co(1)^c	95.16(8)	Co1^a-O4-Co1^c	96.5(1)

Symmetry transformations used to generate equivalent atoms : for **1**, a: 1/4-y, 1/4+x, 9/4-z; b: -x, 1/2-y, z; c: -1/4+y, 1/4-x, 9/4-z; for **2**, a: 5/2-x,3/2-y,z; b: 1/2+y,2-x,-z; c: 2-y,-1/2+x,-z.

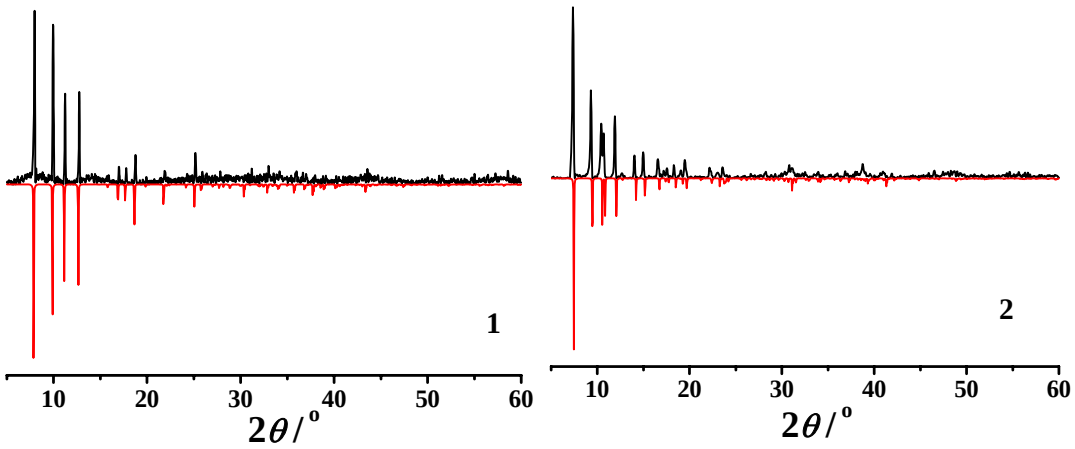

Figure S2. The experimental (black) powder X-ray diffraction and simulated patterns (red) of **1** and **2**.

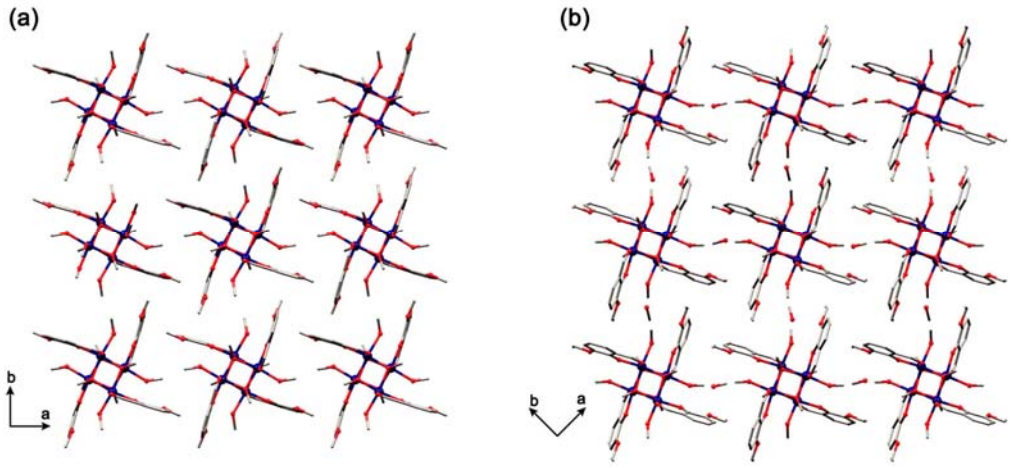

Figure S3. Packing of the molecules in **1** (a) and **2** (b) in the crystal viewed along c-axis within single plane.

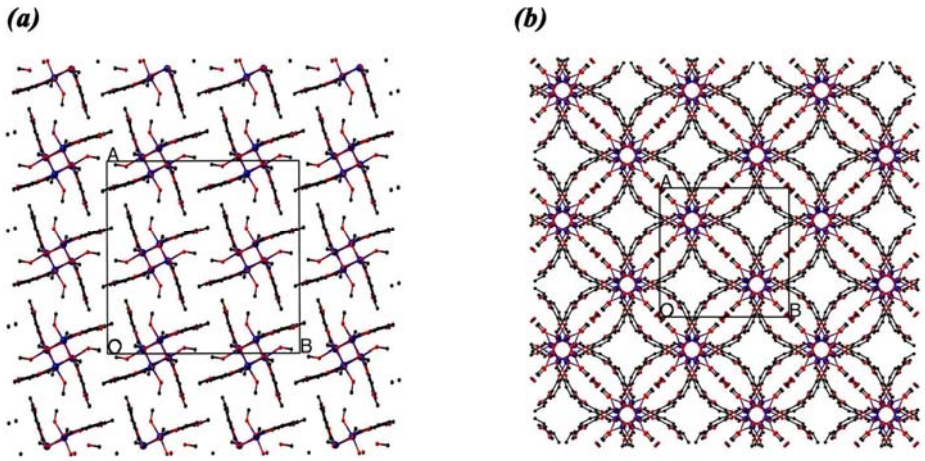

Figure S4. Packing of the molecules of **1** (a) and **2** (b) in the crystal viewed along c-axis for two overlapping planes.

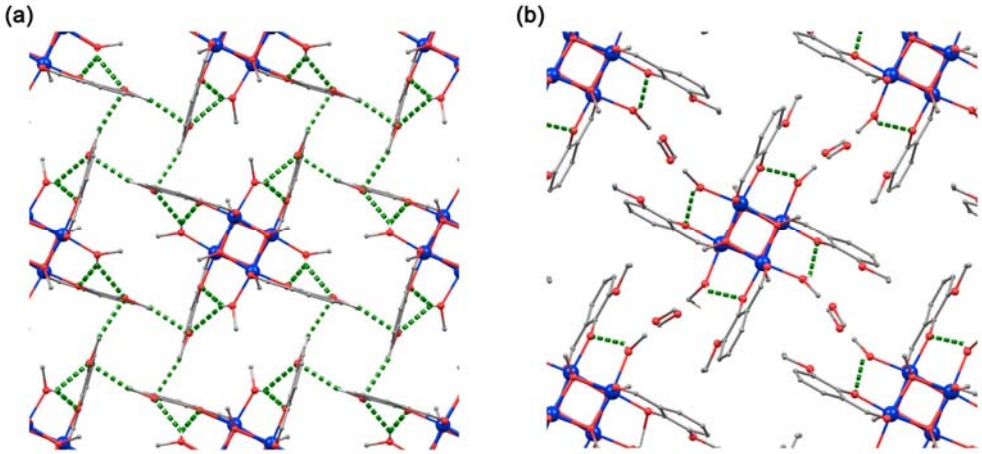

Figure S5. The intra- and inter-cluster H-bonding interactions of **1** and **2**.

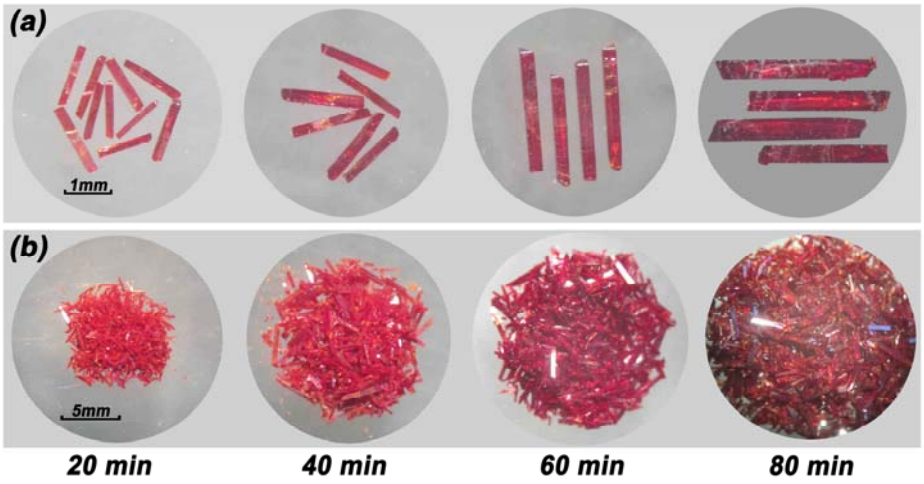

Figure S6. Photos of crystals of **1** for different reaction times by microwave assisted synthesis: (a): local views of single crystals for 20, 40, 60 and 80 min.; (b): total views of the products for 20, 40, 60 and 80 min.

Peak Assignment	Observed *m/z*	Calculated *m/z*
$[Co(hmb)(OH)_3(H_2O)_2+3Na^+]^+$	365.99	365.97
$[Co_2(hmb)_2(OH)_3(H_2O)_3+2Na^+]^+$	570.98	570.96
$[Co_7(hmb)_5(CH_3O)_5(OH)_2]^{2+}$	678.41	678.41
$[Co_7(hmb)_5(CH_3O)_6(OH)]^{2+}$	685.41	685.42
$[Co_4(hmb)_2(OH)_5(H_2O)_8]^+$	766.87	766.91
$[Co_4(hmb)_3(CH_3O)(OH)_3]^+$	770.87	770.87
$[Co_4(hmb)_3(CH_3O)_2(OH)_2]^+$	784.89	784.89
$[Co_4(hmb)_3(CH_3O)_3(OH)]^+$	798.90	798.90
$[Co_4(hmb)_3(CH_3O)_4]^+$	812.92	812.92
$[Co_3(hmb)_4(CH_3O)(CH_3OH)_6(H_2O)]^+$	1022.13	1022.14
$[Co_3(hmb)_4(CH_3O)(CH_3OH)_7]^+$	1036.15	1036.15
$[Co_5(hmb)_4(OH)_5(H_2O)_8]^+$	1127.89	1127.92
$[Co_5(hmb)_4(OH)_5(H_2O)_7(CH_3OH)_2]^+$	1173.93	1173.96

Table S2: Details of major species assigned to the peaks in the ESI-MS spectrum of the methanol solution of **1**.

Peak Assignment	Observed *m/z*	Calculated *m/z*
$[Co(hmb)_2+Na^+]^+$	384.00	384.00
$[Co(hmb)(CH_3OH)_7(H_2O)_4]^+$	506.25	506.19
$[Co_2(hmb)_2(OH)_3(H_2O)_3+2Na^+]^+$	570.98	570.96
$[Co_2(hmb)_3(CH_3OH)(H_2O)_2]^+$	639.00	639.03
$[Co_7(hmb)_5(OH)_7(H_2O)_7]^{2+}$	706.40	706.41
$[Co_7(hmb)_6(CH_3O)_3(OH)_3]^{2+}$	731.41	731.41
$[Co_7(hmb)_6(CH_3O)_4(OH)_2]^{2+}$	738.42	738.42
$[Co_7(hmb)_6(CH_3O)_5(OH)]^{2+}$	745.43	745.43

Table S3: Details of major species assigned to the peaks in the ESI-MS spectrum of the ethanol solution of **1**.

Peak Assignment	Observed *m/z*	Calculated *m/z*
$[Co(heb)(OH)_3(H_2O)_2+3Na^+]^+$	380.01	379.99
$[Co_2(heb)(CH_3O)_3(OH)(H_2O)+2Na^+]^+$	492.97	492.99
$[Co_2(heb)_3]^+$	613.02	613.03
$[Co(heb)_2(CH_3O)(CH_3OH)_2(H_2O)_6+2Na^+]^+$	638.18	638.15
$[Co_7(heb)_6(CH_3O)_4(OH)_2]^{2+}$	780.47	780.47
$[Co_7(heb)_6(CH_3O)_5(OH)]^{2+}$	787.48	787.47
$[Co_4(heb)_3(CH_3O)(OH)_3]^+$	812.91	812.92
$[Co_4(heb)_3(CH_3O)_2(OH)_2]^+$	826.93	826.94
$[Co_4(heb)_3(CH_3O)_3(OH)]^+$	840.95	840.95
$[Co_4(heb)_3(CH_3O)_4]^+$	854.97	854.97
$[Co_3(heb)_4(CH_3O)(CH_3OH)_4(H_2O)_3]^+$	1050.16	1050.17
$[Co_3(heb)_4(CH_3O)(CH_3OH)_5(H_2O)_2]^+$	1064.18	1064.19
$[Co_3(heb)_4(CH_3O)(CH_3OH)_6(H_2O)]^+$	1078.20	1078.20
$[Co_3(heb)_4(CH_3O)(CH_3OH)_7]^+$	1092.21	1092.22

Table S4. Details of major species assigned to the peaks in the ESI-MS spectrum of the methanol solution of **2**.

Peak Assignment	Observed *m/z*	Calculated *m/z*
$[Co_2(heb)_3]^+$	613.02	613.03
$[Co(heb)_2(CH_3O)(CH_3OH)_2(H_2O)_6+2Na^+]^+$	638.18	638.15
$[Co_7(heb)_6(CH_3O)_3(OH)_3]^{2+}$	773.45	773.46
$[Co_7(heb)_6(CH_3O)_4(OH)_2]^{2+}$	780.47	780.47
$[Co_7(heb)_6(CH_3O)_5(OH)]^{2+}$	787.48	787.47
$[Co_4(heb)_3(CH_3O)_4]^+$	854.97	854.97
$[Co_4(heb)_3(CH_3O)_2(CH_3CH_2O)_2]^+$	883.00	883.00
$[Co_4(heb)_4(CH_3O)_2(OH)]^+$	974.98	974.99

$[Co_4(heb)_4(CH_3O)_2(CH_3CH_2O)]^+$	1003.02	1003.02
$[Co_3(heb)_4(CH_3CH_2O)(CH_3OH)_2$ -$(CH_3CH_2OH)(H_2O)_4]^+$	1064.19	1064.19
$[Co_3(heb)_4(CH_3CH_2O)(CH_3OH)_5(H_2O)_2]^+$	1078.21	1078.20
$[Co_3(heb)_4(CH_3O)(CH_3OH)_7]^+$	1092.21	1092.22

Table S5. Details of major species assigned to the peaks in the ESI-MS spectrum of the ethanol solution of **2**.

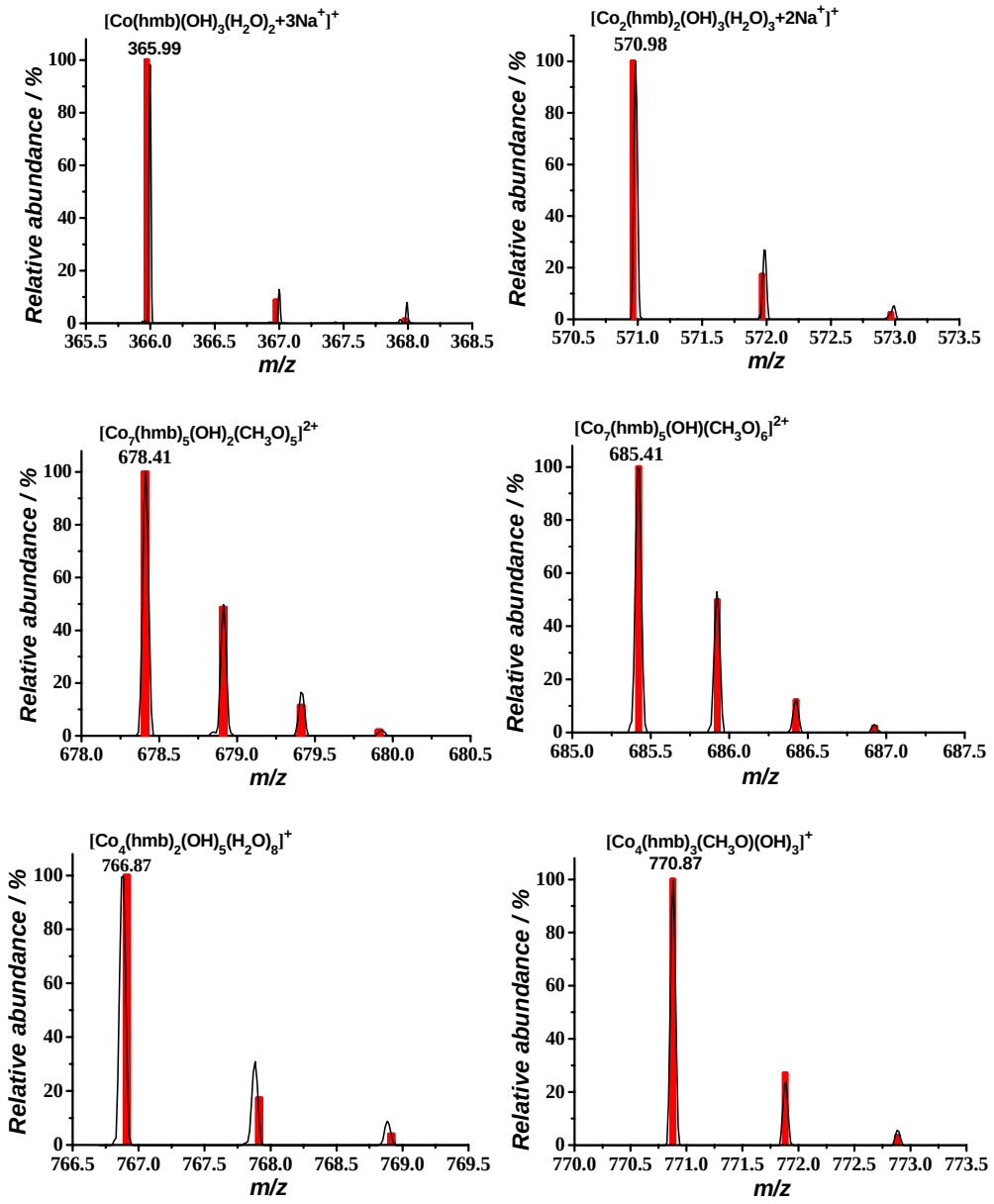

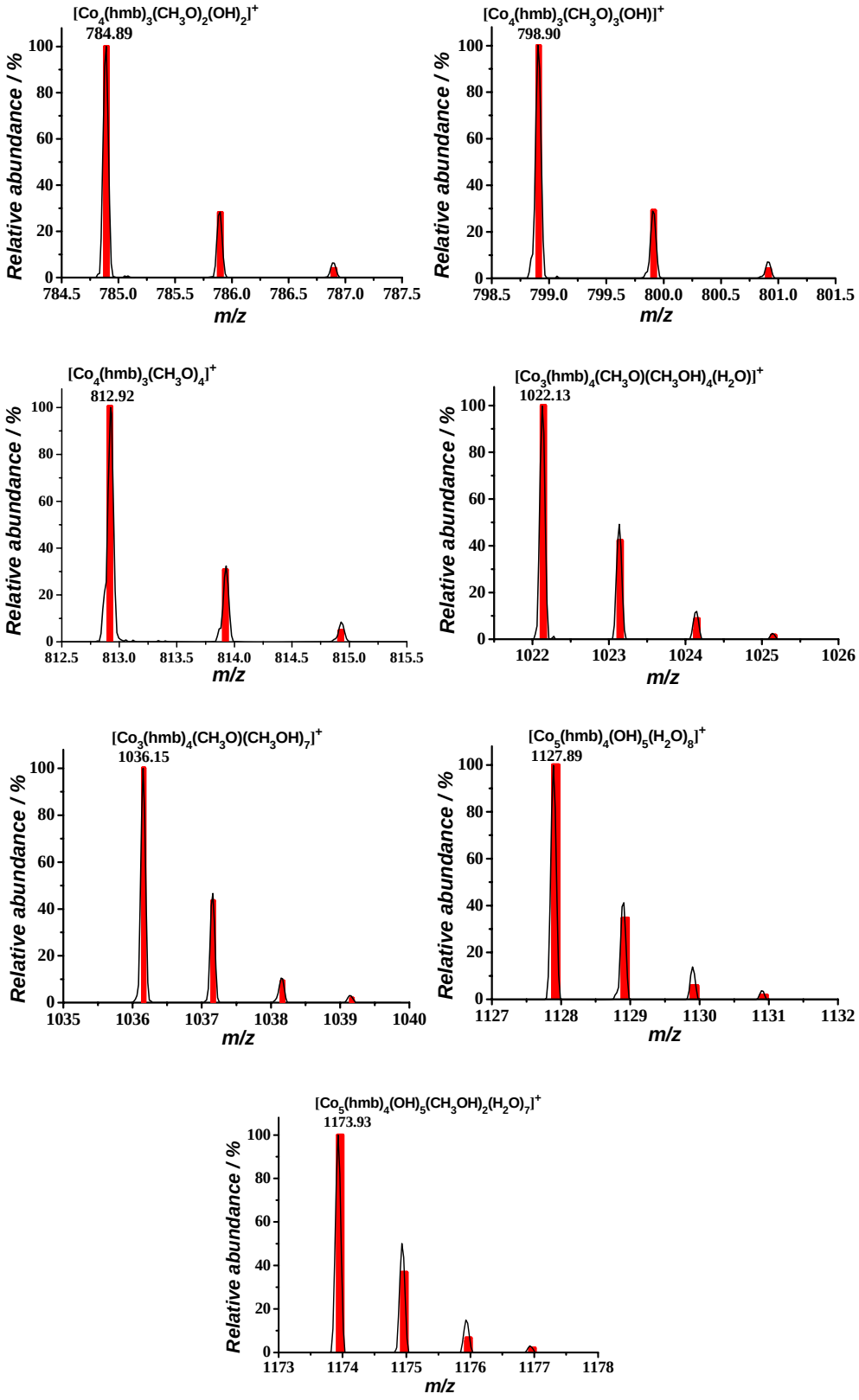

Figure S7. Representation of the calculated peaks fit experimental species present in the ESI-MS spectrum of the methanol solution of **1**. Red bars correspond to the simulated data and black lines correspond to the experimental data.

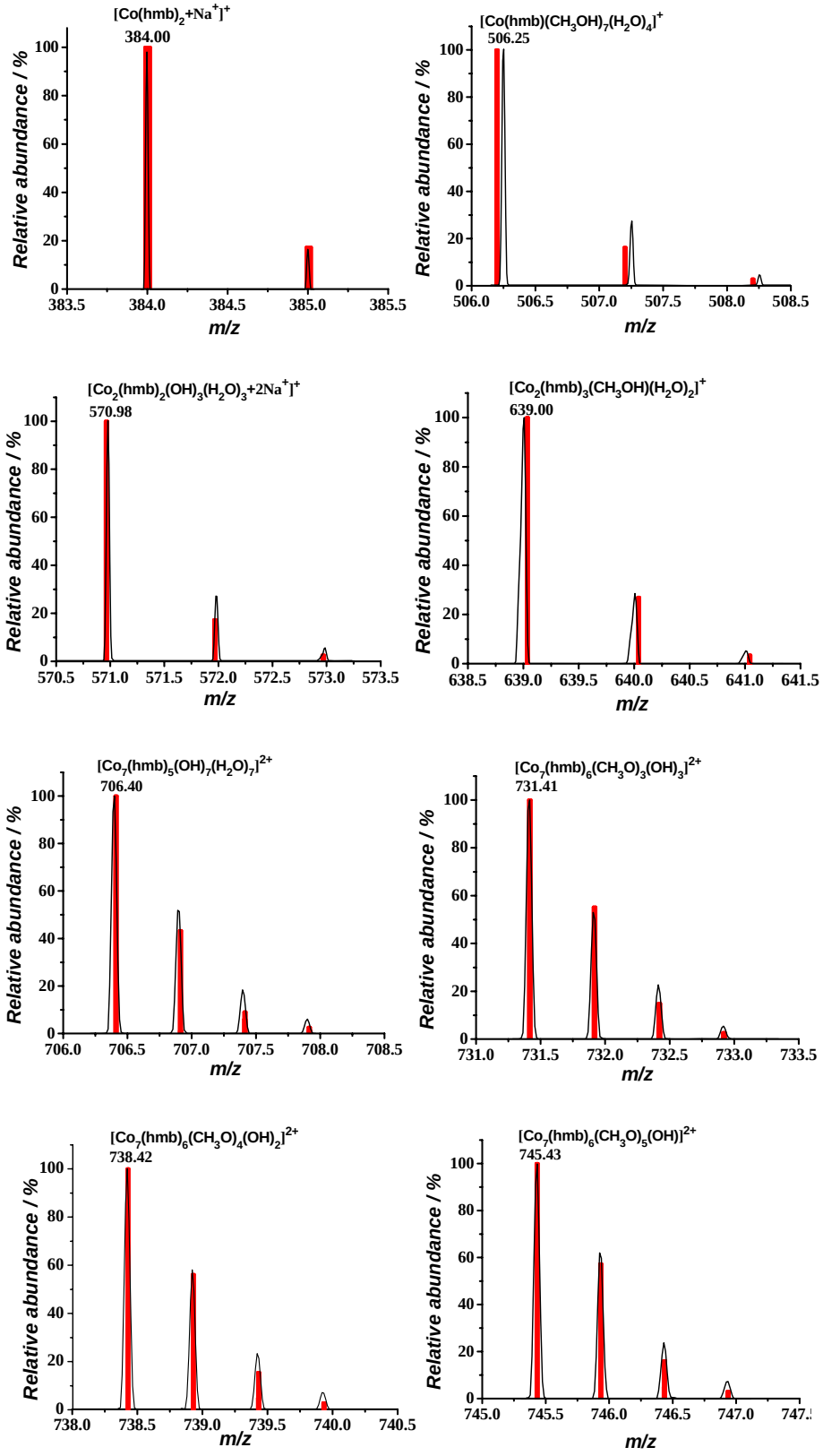

Figure S8. Representation of the calculated peaks fit experimental species present in the ESI-MS spectrum of the ethanol solution of **1**. Red bars correspond to the simulated data and black lines correspond to the experimental data.

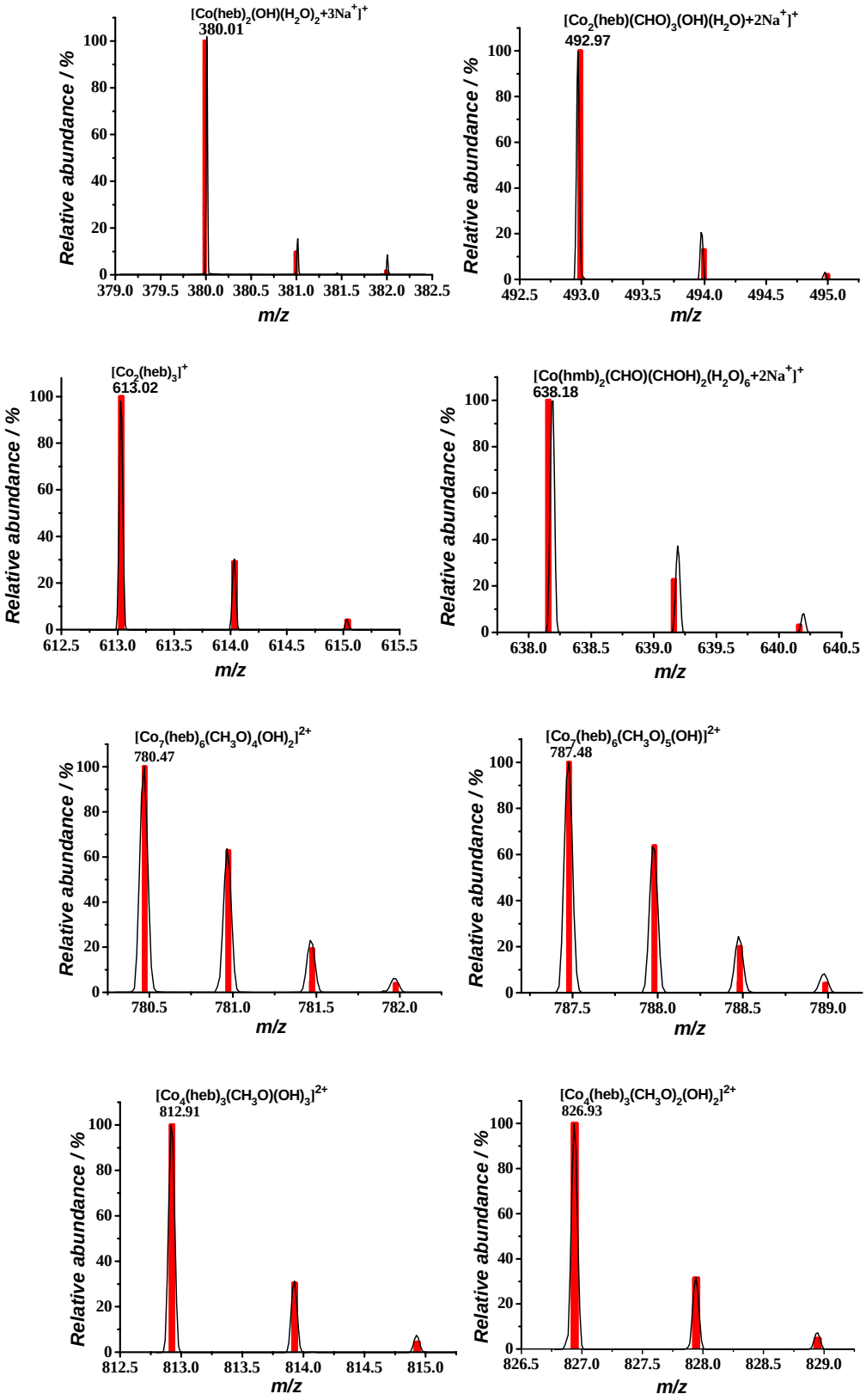

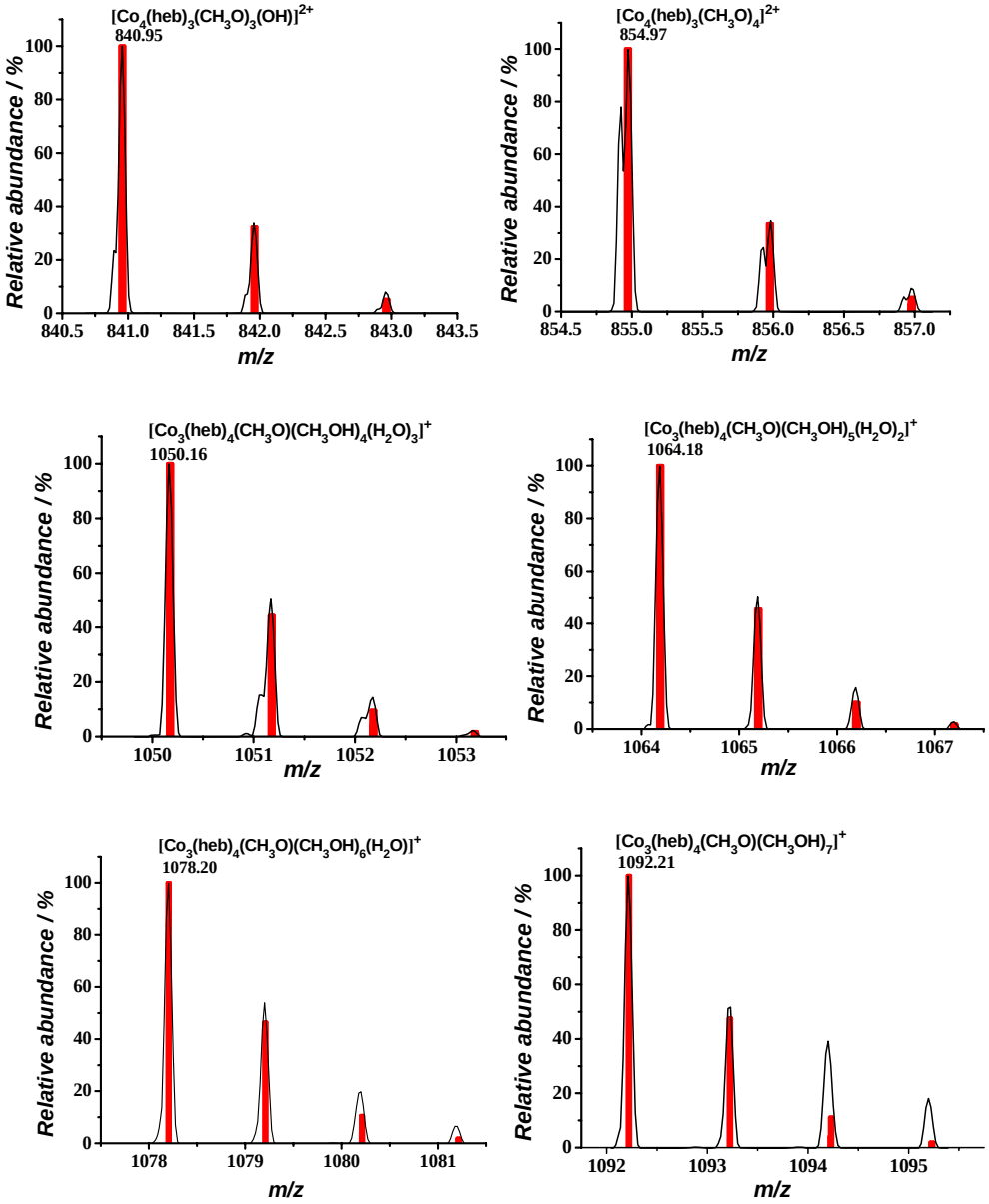

Figure S9. Representation of the calculated peaks fit experimental species present in the ESI-MS spectrum of the methanol solution of **2**. Red bars correspond to the simulated data and black lines correspond to the experimental data.

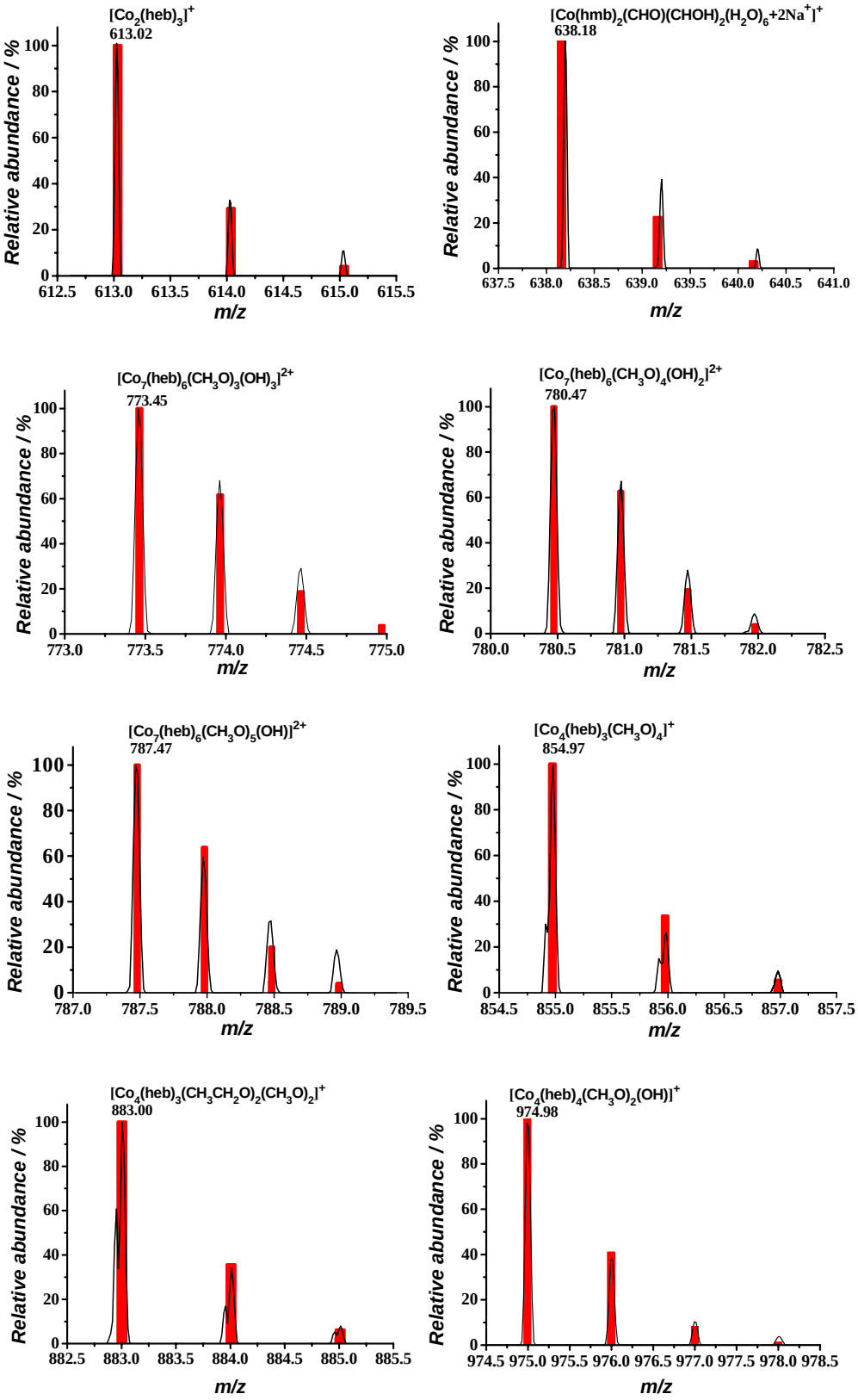

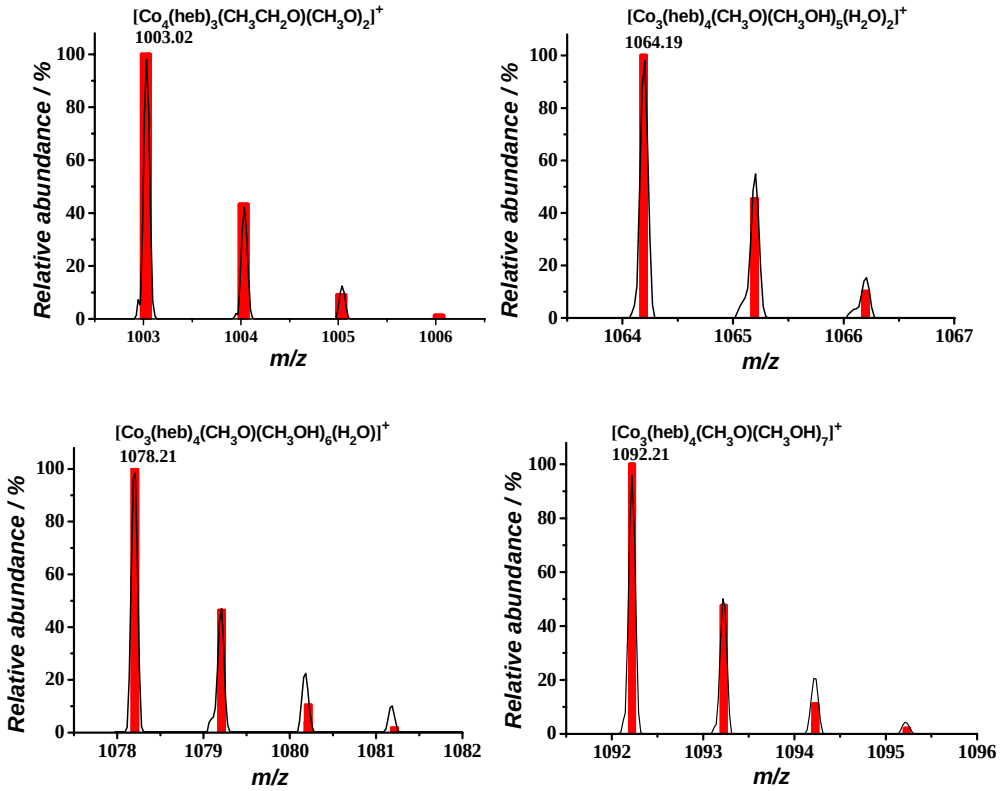

Figure S10. Representation of the calculated peaks fit experimental species present in the ESI-MS spectrum of the ethanol solution of **2**. Red bars correspond to the simulated data and black lines correspond to the experimental data.

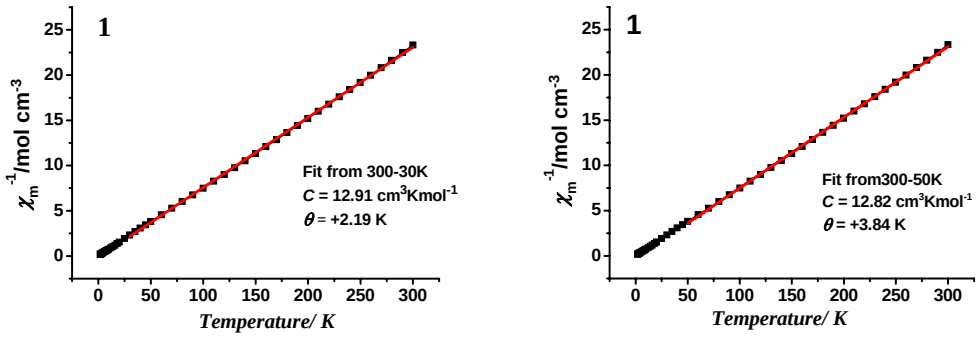

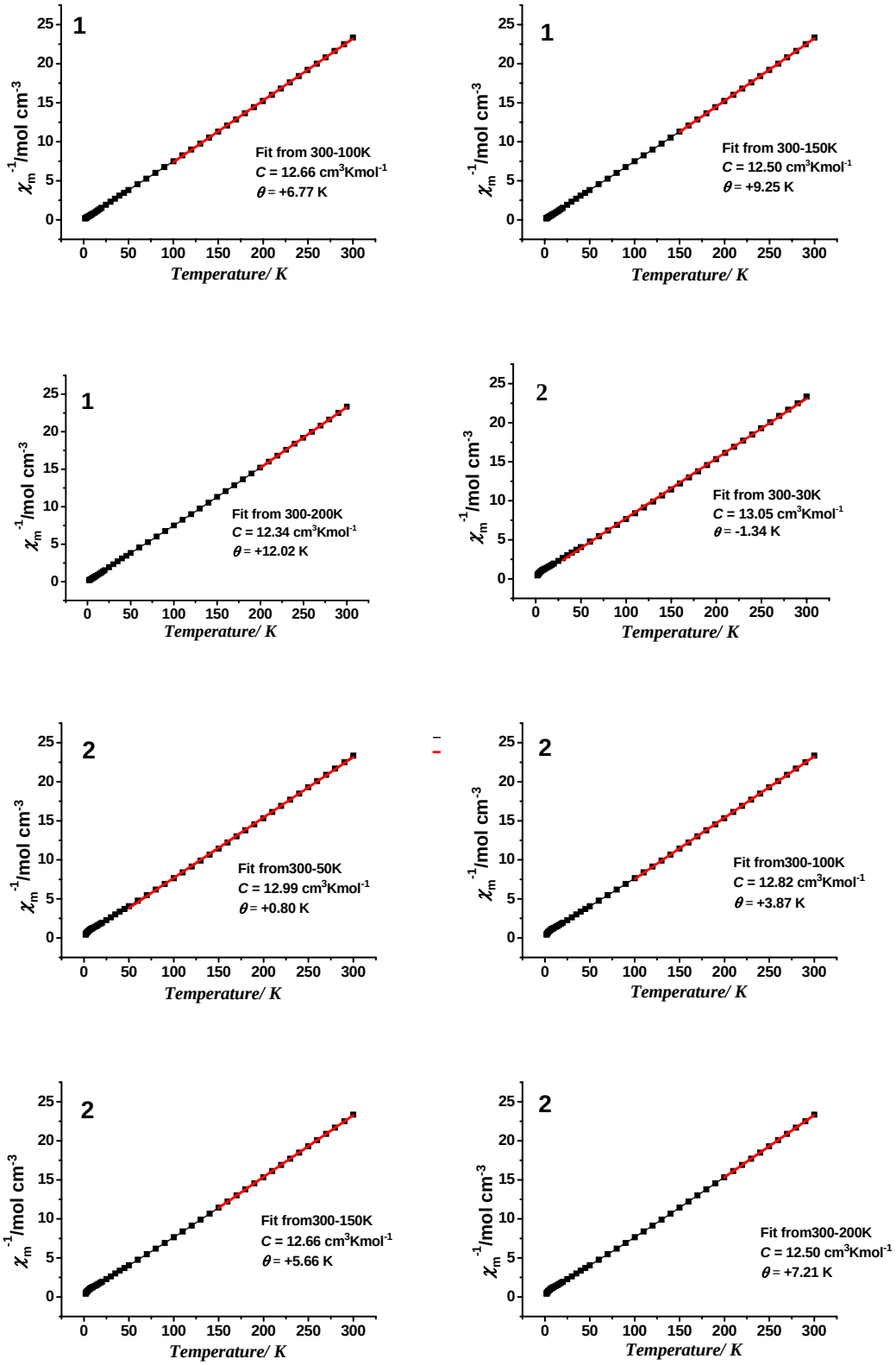

Figure S11. Plots of χ^{-1}_{m} *vs. T* and the fit of Curie-Weiss law (red curve) of **1** and **2** on the different ranges of temperatures.

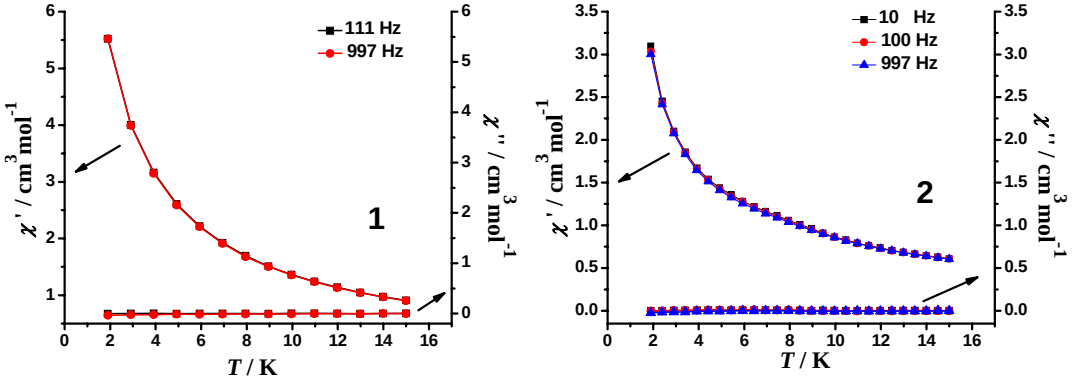

Figure 12. Plots of in-phase (χ') and out-of-phase (χ'') ac susceptibilities for **1** and **2**.